How do glycerol and dimethyl sulphoxide affect local tetrahedral structure of water around a nonpolar solute at low temperature? Importance of preferential interaction

Snehasis Daschakraborty

Citation: The Journal of Chemical Physics **148**, 134501 (2018); doi: 10.1063/1.5019239
View online: https://doi.org/10.1063/1.5019239
View Table of Contents: http://aip.scitation.org/toc/jcp/148/13
Published by the American Institute of Physics

How do glycerol and dimethyl sulphoxide affect local tetrahedral structure of water around a nonpolar solute at low temperature? Importance of preferential interaction

Snehasis Daschakraborty[a)]
Department of Chemistry, Indian Institute of Technology Patna, Patna-801103, Bihar, India

(Received 12 December 2017; accepted 12 March 2018; published online 2 April 2018)

Glycerol and dimethyl sulphoxide (DMSO) have vital roles in cryoprotection of living cells, tissues, etc. The above action has been directly linked with disruption of hydrogen (H-) bond structure and dynamics of water by these cosolvents at bulk region and around various complex units, such as peptide, amino acid, protein, and lipid membrane. However, the disruption of the local structure of the water solvent around a purely hydrophobic solute is still not studied extensively. The latter is also important in the context of stabilization of protein from cold denaturation. Through all-atom molecular dynamics simulation, we have investigated the comparative effect of glycerol and DMSO on the orientational order of water around a nonpolar solute at −5 °C. A steady reduction of the tetrahedral order of water is observed at bulk (>10 Å distance from the solute) and solute interface (<5.5 Å distance from the solute) with increasing the cosolvent concentration. Contrasting roles of glycerol and DMSO have been evidenced. While DMSO affects the H-bond structure of the interfacial water more than that of the bulk water, glycerol affects the water structure almost uniformly at all regions around the solute. Furthermore, while glycerol helps to retain water molecules at the interface, DMSO significantly reduces the water content in that region. We have put forward a plausible mechanism for these contrasting roles of these cosolvents. The solute-cosolvent hydrophobic-interaction-induced orientational alignment of an interfacial cosolvent molecule determines whether the involvement of the cosolvent molecules in H-bonding with solvent water in the interface is akin to the bulk region or not. *Published by AIP Publishing.* https://doi.org/10.1063/1.5019239

I. INTRODUCTION

Cosolvents, like glycerol and dimethyl sulphoxide (DMSO), in liquid water protect living cells and tissues by preventing freezing of water at extremely low temperature. Thus the cosolvents are popularly called as cryoprotectants, and the process of prevention from freezing is known as cryopreservation. Several experimental and computer simulation studies indicated that the anti-freezing action of these cryoprotectants stems from their abilities in disrupting the three-dimensional tetrahedral H-bonding network and underlying molecular dynamics (MD) of liquid water.[1–21] It was observed that the hydroxyl groups of glycerol molecules form strong H-bonds with water and the hydrophobic residues aggregate together. Thereby the regular three-dimensional H-bond network of water is severely disturbed. However, the scenario can be astonishingly different at molecular length scale. For example, it was reported that water forms lower density, more ordered tetrahedral water structure in high glycerol concentration than pure water at room temperature.[2–4] This might be due to the nano-segregation of glycerol-rich and water-rich regions in the mixture, which protects water to form a low-density by an extensive and encapsulating glycerol interface. Multiple experimental and simulation reports indicated similar disruption of three-dimensional H-bonding of water in the presence of DMSO.[5–10,15,16,19–21]

Notwithstanding the fact that the above studies provide a broad view on structural and dynamical perturbation of water by these cosolvents at the bulk regime, they offer limited insight on how these cryoprotectants affect water H-bonding structure and dynamics near a purely hydrophobic solute. The latter is particularly important in understanding the mechanism of protection of proteins by these cosolvents from cold denaturation. The cold denaturation is often linked with the weak hydrophobic interaction among the hydrophobic residues of protein at low temperature.[22–49] However, the increased H-bond interaction between polar residues of amino acid and solvent water at low temperature may also play an important role in cold denaturation of protein.[50–52] Apart from the above two pictures, another exciting view also exists. A Monte Carlo simulation-based approach indicated that the increase of water· · · water H-bonding at the protein interface with lowering of temperature is the sufficient condition for protein's cold denaturation.[53] We will return to this discussion again in Sec. III.

Some reports are found in the literature on how glycerol and DMSO affect the water solvent structure and dynamics near peptide, amino acid residues, protein, lipid membrane, etc. It was found that both the cosolvents substantially perturb water solvent structure and dynamics near all the above entities. However, the mechanisms of the above actions of these

[a)]Author to whom correspondence should be addressed: snehasis@iitp.ac.in

two cosolvents are notably different. The MD simulation study by Johnson *et al.* has analyzed the role of the two cosolvents in peptide hydration structures.[54] While the presence of glycerol in the solution increases hydration number near the peptide interface, DMSO effectively reduces it. Similar contrasting behavior was seen on the lipid membrane interface.[55] Glycerol influences the diffusivity of water almost uniformly near the bilayer surface and that in the bulk solution, but DMSO increases the diffusivity of surface water more than that of the bulk water molecules. It is also known that glycerol and DMSO act very differently for stabilization of protein. Glycerol is an excellent protein stabilizer,[54,56,57] whereas DMSO's action is diverse and strongly dependent on the concentration of DMSO in the solution.[58–64] For example, with increasing DMSO concentration, initially (at $x_D < 0.05$) the conformational flexibility of lysozyme increases, followed by the slight unfolding of native state in the DMSO concentration range $0.10 < x_D < 0.15$, and finally unfolding of the protein after $x_D > 0.15$.[58] This picture was later supported by an MD simulation study.[62]

Although the above studies provide significant insights on some specific questions, a more fundamental question remains mostly unaddressed. The question is, how do these cosolvents affect the strong H-bonding clathrate like cage structure of water[65,66]—popularly known as "iceberg," first proposed by Frank and Evans and later evidenced by several experimental and computer simulation studies[67–73]—around a purely hydrophobic solute?

We have studied here the effect of glycerol and DMSO concentration on the orientational ordering of solvent water molecules around a very simple nonpolar solute, xenon (Xe) using classical MD simulation. It is well known that Xe is prototypical hydrophobic solute and its hydration structure and dynamics in liquid water resemble other popularly known hydrophobic solutes, like methane and ethane.[67,73–77] However, one can still ask whether the influence of the cosolvents on the hydration structure around the small nonpolar solute, Xe, is analogous to the influence on the hydration structure around much more complicated and bigger entities, such as protein and lipid membrane. It was observed earlier that the hydration structure around a hydrophobic solute changes significantly with an increase in the size of the solute.[78–84] The pioneering Lum-Chandler-Weeks theory predicts that for small solutes the free energy of hydration of a hard-sphere solute increases almost linearly with the solute volume but beyond a critical length scale (also termed as small-to-large crossover length scale) the free energy increases linearly with the surface area of the solute.[78] The theory, therefore, predicts drying of the extended nonpolar surface only beyond the small-to-large crossover length scale (~1 nm) of the nonpolar solute.

A molecular simulation was also carried out to study the effect of various thermodynamic properties and concentration of additive, like ethanol, on the above small-to-large crossover length scale.[81] (Note that this length scale is ~1 nm under standard temperature and pressure condition.) It was found that the crossover length scale can decrease up to the size of a small molecule after adding ethanol like cosolvent. This is very important in the context of the present study because we have also used the cosolvents, glycerol or DMSO, which are not very different from ethanol regarding interaction with water. Therefore we expect a decrease of the small-to-large crossover distance to the size of the small solute, like Xe, for the mixtures. Our choice of the solute in the present study is further emboldened by a recent molecular simulation study,[85] which intended to elucidate whether proteins behave effectively like small or large non-polar solute (in terms of the hydrophobic effect). The simulation has reported the following observation. Despite the proteins are large units (larger than 1 nm), they can behave effectively like "small" particles (i.e., smaller than 1 nm) in terms of hydrophobic effect. The complex structure of proteins, having both polar and non-polar residues, is the possible reason for the above behavior. Therefore, the proximity of polar and nonpolar residues in protein makes protein hydration structure very similar to small nonpolar solute, which influences the solvent water H-bonding strength only slightly. Therefore, we expect that the observation for the system can be transferred to systems of practical interest for understanding the role of cryoprotectants in influencing the hydrophobic structure.

The simulation was done at 268 K temperature given the interest in the cosolvent activity at that temperature around what cold denaturation often occurs for various proteins. In this study, we are asking the following questions: How do these two cosolvents perturb the local tetrahedral structure of water around the solute? Do the cosolvents uniformly affect the structure of water inside and outside the first hydration shell? Are there any contrasting effects of glycerol and DMSO on hydrophobic hydration structure? Is there any role of preferential solvation?

The outline for the remainder of this paper is as follows. The molecular models and other simulation details are detailed in Sec. II. Section III presents the simulation results and discussions. Concluding remarks are offered in Sec. IV.

II. SIMULATION DETAILS

In order to study the composition dependence of the results, we have considered here 6 compositions (with the mole fraction of glycerol or DMSO, x = 0.02, 0.05, 0.07, 0.10, 0.12, and 0.15) for each of the glycerol+water (GW) and DMSO+water (DW) mixtures plus neat liquid water, resulting in total 13 different systems. We have not gone beyond the mole fraction of the cosolvent $x = 0.15$ because of the following reason. Although protein is stable at a far wide range of compositions of GW mixtures (including $x_G = 0.99$!),[86] the former is stable only at a narrow range of composition in the DW mixture. It was observed that lysozyme starts denaturing beyond $x_D = 0.15$ mole fraction of DMSO in the DW mixture.[58–64,87] Therefore, we have limited our studies up to the composition, $x = 0.15$, where the protein stays stable in its native state.

All-atom modeling of glycerol molecules are done using AMBER[88] type force field parameters, initially developed by Chelli *et al.*[89] and later modified by Blieck *et al.*[90] The TIP4P/2005 model[91] has been used for water molecules. This combination of the force field models is proven to be the most successful in reproducing experimental thermodynamic

properties and other microscopic structural and transport properties of the GW binary mixture at a wide range of temperatures including sub-zero.[92] We have used here the fully atomistic Strader-Feller model of DMSO,[93] which is highly successful in predicting experimentally observed thermodynamic and microscopic quantities. The nonpolar solute Xe is modeled as 12-6 Lennard-Jones (LJ) particle having LJ parameters used elsewhere.[74,75] The solute–solvent cross parameters are deduced from the Lorentz–Berthelot mixing rules, which is the best combination rule for the aqueous solution of Xe.[76]

First, we optimized a glycerol and a DMSO molecule separately in the gas phase at the B3LYP/6-311+G** level of theory[94,95] and basis set using the Gaussian 09 package.[96] Then we prepared 13 simulation boxes—each having box length of 30 Å—by mixing an appropriate number of geometrically optimized glycerol and DMSO molecules separately with water following the composition of the solvent mixture and one Xe solute. Each simulation box contains 500 solvent molecules and 1 solute molecule. The initial configurations of the molecules were set up randomly using the PACKMOL software.[97] The compositions of the mixtures have been detailed in Table S1 of the supplementary material.

MD simulations for the above 13 systems were then initiated using the Gromacs software package.[98] All the systems were first equilibrated using the NPT ensemble for 10 ns. The temperature was maintained at 268 K using the Nośe-Hoover thermostat (coupling time 0.5 ps)[99,100] and pressure at 1 bar using the Berendsen barostat (coupling time 0.5 ps).[101] In order to confirm that the Berendsen barostat is working correctly—specifically, whether the resulting density of the system remains same on using different pressure coupling methods[102]—we re-equilibrate the systems with the Parrinello-Rahman barostat[103] with the same coupling constant of 0.5 ps. The equations of motions were always solved using the Verlet leapfrog algorithm every after 1 fs. Table S1 of the supplementary material lists the final simulated densities separately for the above two barostats. Clearly, the final densities are almost the same, indicating consistent density equilibration with the two barostats. Also, the final densities are in excellent agreement with earlier simulation and experimentally measured densities.[92,104] This further supports our choice of force field models for the solvent molecules and other simulation parameters.

For obtaining production trajectories, NVT simulations were initiated from the final configurations of the previous NPT simulations. These simulations were run for 40 ns by solving equations of motion every after 1 fs using the Verlet leapfrog algorithm. The temperature constraining was done by using the Nośe-Hoover thermostat, one of the efficient temperature control algorithms,[102] at 268 K with a coupling constant of 0.5 ps. The configurations were saved after every 50 fs time for analysis. The above simulation protocols are akin to other relevant simulation studies.

III. RESULTS AND DISCUSSIONS

In this section, we first discuss the consequence of increasing glycerol and DMSO concentration in aqueous solution on the local tetrahedral order of liquid water around the hydrophobic solute. We continue our discussion in Subsections III B–III C about the roles of these two cosolvents in H-bonding and spatial structure of water solvent around the solute. Finally, we illustrate the observations by looking at the orientational arrangement of the cosolvent molecules in the hydration shell of the Xe solute.

A. Tetrahedral order parameter

Orientational tetrahedral order parameter (q) is the most extensively used parameter for understanding the tetrahedral structure of a liquid. (See, e.g., Refs. 67 and 105–110.) For neat liquid water, q is calculated by considering 4 nearest water oxygen (O_W) atoms from a central water O_W and using the following equation:

$$q = 1 - \frac{3}{8}\sum_{j=1}^{3}\sum_{k=j+1}^{4}\left(\cos\theta_{jk} + \frac{1}{3}\right)^2. \quad (1)$$

Here, θ_{jk} is the angle formed by the lines joining O_W of a given water molecule and those of its four nearest neighbors j and k. For entirely random configuration, like an ideal gas, the average value $\langle q\rangle$ is 0. On the other hand, $\langle q\rangle = 1$ for perfectly tetrahedral configuration, like ice.

First, we study q for water clusters in the two mixtures. Figures 1(a) and 1(c) present the normalized probability density distributions of q for pure water, 3 GW mixtures ($x_G = 0.05$, 0.10, and 0.15), and 3 DW mixtures ($x_D = 0.05$, 0.10, and 0.15). In this calculation, we have considered only the nearest four water molecules from a central water molecule. The rationale is to check how the cosolvents prevent tetrahedral ordering of water among themselves around the hydrophobic solute at low temperature. q is calculated for 1st hydration shell (interfacial) and bulk water molecules separately. The interface and the bulk are identified from radial distribution function (RDF) between the solute Xe and water O_W, presented in Figs. S1 and S2 of the supplementary material. The interfacial layer extends up to 5.5 Å distance from the solute (position of the first minima of Xe—O_W RDF). The space outside 10 Å distance from the solute (Xe—O_W RDF almost levels off after this distance) is considered as bulk. Note that these distance criteria are consistent with a recent MD simulation study.[111] Figures 1(a) and 1(c) show that the distribution of q—both at interface and bulk—is maximum at $q \sim 0.83$ with a shoulder at $q \sim 0.50$ for pure water. The local tetrahedral structure of water at the present simulation temperature (T = 268 K) is palpably more ordered than the structure at T = 298 K.[67,110] The intensity of the peak for both the interfacial and bulk water decreases steadily. (As suggested in Ref. 53, this low-temperature ordering of solvent water near nonpolar solute can be the key for cold denaturation of the protein.) However, no significant shift of the peak is observed. Closer inspection of Figs. 1(a) and 1(c) further reveals that while the intensity of the peak—centered at $q \sim 0.83$—gradually decreases, new peak burgeons at $q \sim 0.45$. The intensity of the new peak prevails over the intensity of the peak at $q \sim 0.83$ beyond $x = 0.10$.

In order to elucidate further, we view the structures of 5 water clusters including the central water for $q \sim 0.83$ and

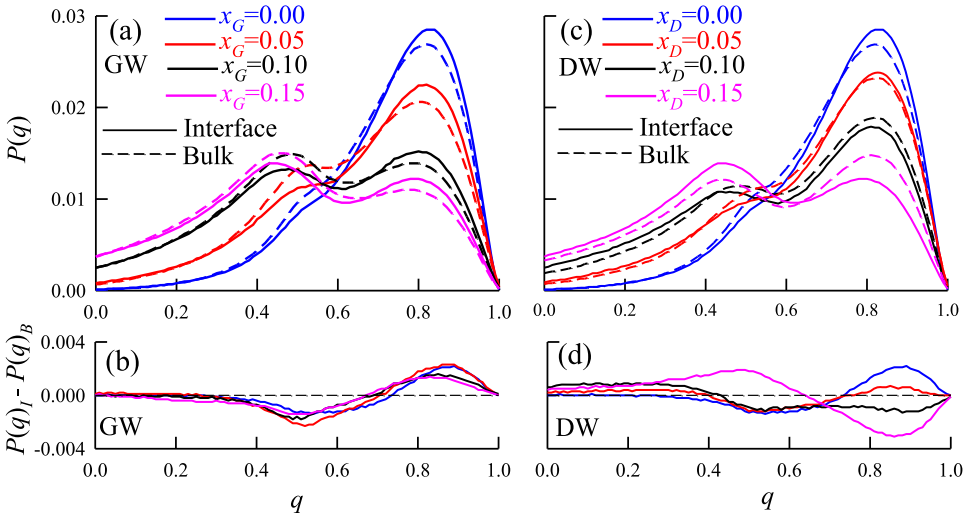

FIG. 1. Normalized probability distribution of the tetrahedral order parameter, q, for bulk (dashed lines) and interfacial water molecules (solid lines) for neat water and binary mixtures of water and cosolvents at different compositions: (a) GW mixtures and (c) DW mixtures. Difference between the distributions of q in bulk and the first hydration shell around the solute for (b) GW and (d) DW binary mixtures.

$q \sim 0.45$ for both GW and DW mixtures. Four such water clusters are shown in Fig. 2. Apparently, the structures in Figs. 2(a) and 2(b) are close to the regular tetrahedron. Therefore, the peak at $q \sim 0.83$ corresponds to a tetrahedral-like arrangement with the four water molecules situated at the four vertices of the tetrahedron. On the other hand, Figs. 2(c) and 2(d) reveal that the peak at $q \sim 0.45$ corresponds to a broken tetrahedral geometry with one water molecule dislocated from one vertex of the tetrahedron. This essentially suggests that the gradual burgeoning peak at $q \sim 0.45$ with increasing glycerol/DMSO concentration—in Figs. 1(a) and 1(c)—is due to the disruption of the local tetrahedral geometry of water at both the bulk and hydrophobic interface. At $x > 0.10$, the water clusters turn out to be dominated by the distorted tetrahedral structure. We will show later that the fourth free vertex of the tetrahedron is actually occupied by a cosolvent molecule and thereby uphold "hybrid" tetrahedral clusters (composed of both water and cosolvent molecules) around the center water molecule.

Now, we turn our focus on comparative analysis between the distributions of q for interfacial and bulk water molecules. The differences between the two distributions are shown in Figs. 1(b) and 1(d) for GW and DW mixtures, respectively. For pure water, the tetrahedral structure of interfacial water solvent is more ordered than that of the bulk. This is consistent with the picture that the strong H-bonding structure of interfacial water exists in the vicinity of the hydrophobic solute.[67–73] Figures 1(a) and 1(c) demonstrate that even though the tetrahedral orders of both the bulk and interfacial water molecules decrease with increasing mole fraction of glycerol in the GW mixtures, the interfacial water molecules always stay more ordered than bulk water. However, the picture is markedly different for DW mixtures. The interfacial water molecules become eventually less ordered than the bulk waters at $x_D > 0.05$ for DW mixtures.

To elucidate further with the more quantitative analysis, we plot average tetrahedral order parameters of the interfacial water molecules ($\langle q_I \rangle$) and those of the bulk water molecules

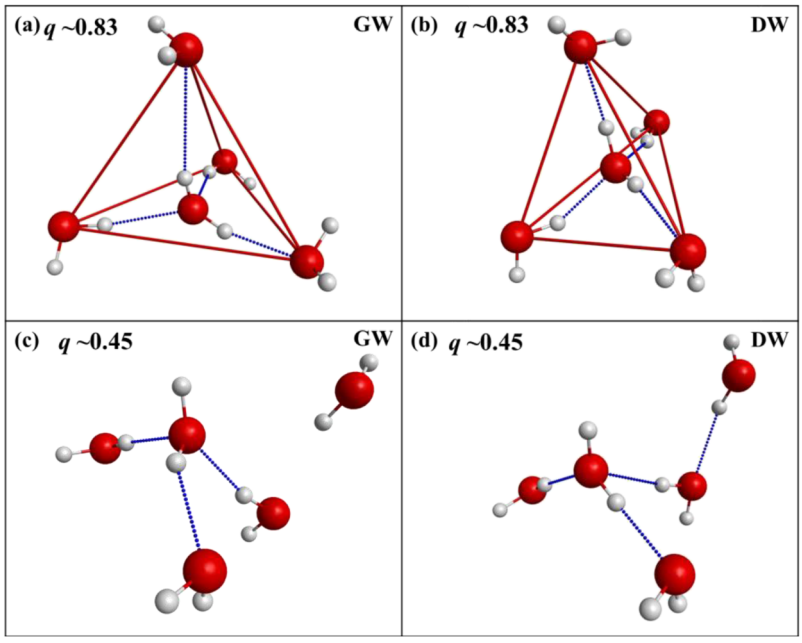

FIG. 2. Representative water clusters for $q \sim 0.83$ and $q \sim 0.45$ for GW and DW binary mixtures.

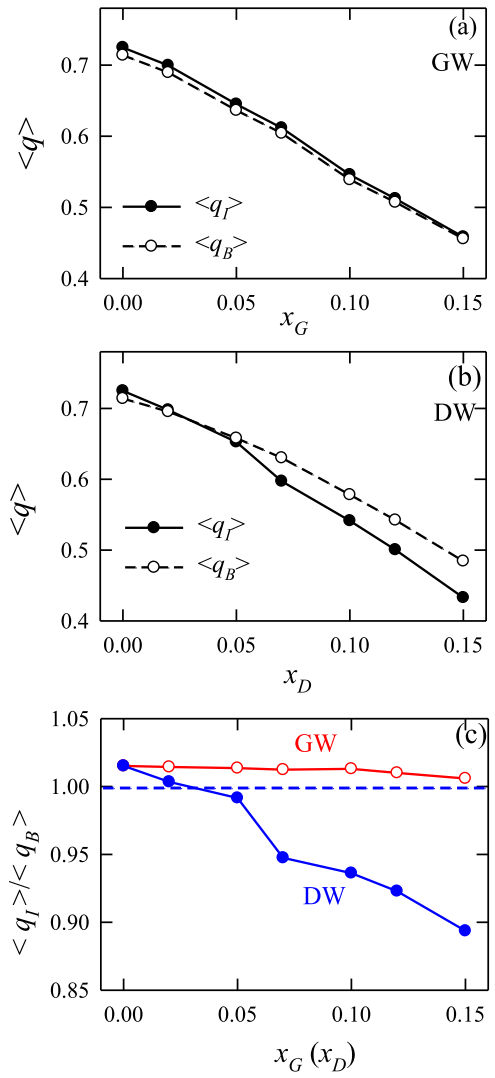

FIG. 3. Average tetrahedral order parameters of the interfacial water molecules ($\langle q_I \rangle$) (solid line with filled circles) and those of the bulk water molecules ($\langle q_B \rangle$) (dashed line with open circles) in the two mixtures: (a) GW and (b) DW as a function of x_G and x_D, respectively. (c) The ratios $\langle q_I \rangle / \langle q_B \rangle$ as functions of x_G and x_D for the two mixtures. The red line with open circles and the blue line with filled circles represent for GW and DW mixtures, respectively, in panel (c). Horizontal dashed blue line in panel (c) indicates $\langle q_I \rangle / \langle q_B \rangle = 1$.

($\langle q_B \rangle$) for GW and DW mixtures in Figs. 3(a) and 3(b), respectively. Evidently, both $\langle q_I \rangle$ and $\langle q_B \rangle$ decreases almost linearly with increasing the cosolvent concentration. The ratio $\langle q_I \rangle / \langle q_B \rangle$ is plotted in Fig. 3(c) as functions of x_G and x_D for GW and DW mixtures, respectively. The ratio $\langle q_I \rangle / \langle q_B \rangle$ is above unity for all the compositions of the GW mixtures and stays almost insensitive on glycerol concentration up to $x_G = 0.15$, the maximum glycerol concentration in the present study. This immediately suggests that glycerol uniformly affects the interfacial and bulk water. However, the scenario is entirely different for DW mixtures. Figure 3(c) shows that $\langle q_I \rangle$ decreases more rapidly than $\langle q_B \rangle$ with increasing x_D in DW mixtures. Therefore the ratio $\langle q_I \rangle / \langle q_B \rangle$ becomes less than unity at $x_D > 0.05$ and decreases up to a value of 0.9 at $x_D = 0.15$. This suggests that, unlike glycerol, DMSO affects the tetrahedral arrangement of the interfacial water more radically than that of the bulk water. The observation that glycerol uniformly influences the tetrahedral structure of water around the hydrophobic solute and that DMSO disrupts the tetrahedral arrangement of interfacial water more drastically than that of the bulk water strongly recommends the contrasting roles of these two cosolvents in affecting the tetrahedral structure of water around a hydrophobic solute. Similar contrasting behaviors of these two cosolvents were reported earlier while studying the effect of these cosolvents on hydration structure and dynamics near the peptide water interface.[54] While glycerol increases the hydration number near the peptide interface, DMSO decreases the hydration number near the same peptide interface. This might be due to the preferential hydration of the hydrophobic residues. We will return to this discussion in Sec. III B. A more recent experimental study has also revealed that DMSO and glycerol affect the diffusivity of interfacial and bulk water (from lipid bilayer surface) very differently.[55] While glycerol uniformly affects the diffusivity of water irrespective of the distance from the lipid bilayer surface, DMSO significantly increases the diffusivity of surface water compared to that of the bulk water.

Now, we turn our focus on how glycerol and DMSO cosolvents directly participate in the local tetrahedral structure of liquid water. While glycerol molecules can act as both the H-bond donor and acceptor with water solvent molecules, DMSO molecules only accept H-bonds from the solvent water. In the beginning of this section, we have indicated that one vertex—in majority of the tetrahedral clusters of water around the hydrophobic solute—turns out to be liberated from water when the mole fraction of the cosolvent reaches $x = 0.15$ and that a cosolvent molecule occupies this unattended position by forming H-bond with the central water solvent molecule. Figures 4(a) and 4(b) present the normalized probability density distributions of q for pure water, 3 GW mixtures ($x_G = 0.05$, 0.10, and 0.15), and 3 DW mixtures ($x_D = 0.05$, 0.10, and 0.15). In this calculation, we have considered the nearest four solvent molecules (both water and cosolvents) from a central water molecule. Clearly, the distributions for both GW and DW mixtures culminate at $q \sim 0.8$ with a shoulder at $q \sim 0.5$. Unlike in Fig. 1, the peak of the distribution remains fixed at $q \sim 0.8$ for all compositions and no new peak emerges at $q \sim 0.5$ except there is a slight rise of the shoulder. Clearly, the peak intensity decreases with increasing cosolvent concentration. However, the loss of the peak intensity is much less than when only water clusters are considered in the calculation. This indicates that the retention of the tetrahedral structure occurs at least up to $x = 0.15$. However, the pure water tetrahedral clusters turn into the multicomponent tetrahedral cluster. These "hybrid" tetrahedral structures may potentially reduce the probability of ice crystal formation and their growth. These observations support the fact that these cosolvents act as potential anti-freezing substances.[1–21]

We have presented, in Figs. 5(a) and 5(b), the average tetrahedral order parameters $\langle q_I \rangle$ and $\langle q_B \rangle$ for the interfacial and bulk water solvent molecules, respectively, in DW and GW mixtures. These are calculated for the tetrahedral clusters composed of both water and cosolvents. Figure 5(a) shows that both the $\langle q_I \rangle$ and $\langle q_B \rangle$ decrease almost parallel with increasing x_G. Naturally, the ratio $\langle q_I \rangle / \langle q_B \rangle$ remains almost constant

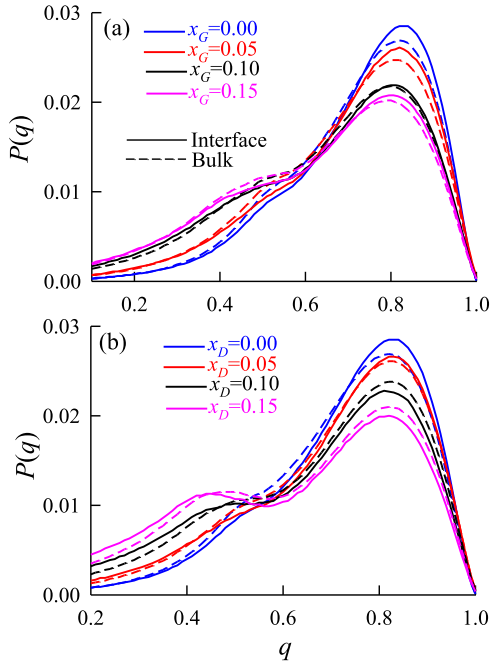

FIG. 4. Distribution of the tetrahedral order parameter, q, for bulk (dashed lines) and interfacial water molecules (solid lines) for neat water and binary mixtures of water and cosolvents at different compositions: (a) GW mixtures and (b) DW mixtures. Note that these calculations are done by considering the nearest four solvent molecules (both water and cosolvents) from a central water molecule.

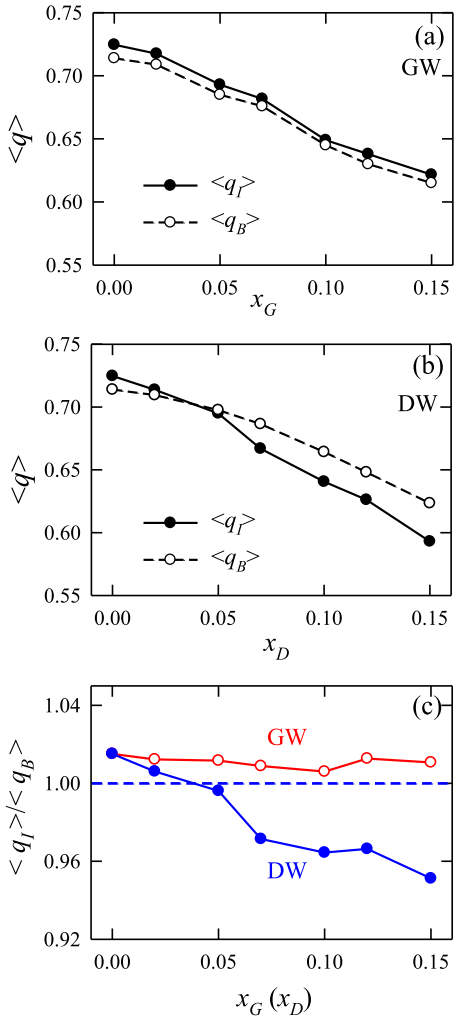

FIG. 5. Average tetrahedral order parameters of the interfacial water molecules ($\langle q_I \rangle$) (solid line with filled circles) and of the bulk water molecules ($\langle q_B \rangle$) (dashed line with open circles) in the two mixtures: (a) GW and (b) DW as a function of x_G and x_D, respectively. (c) The ratios $\langle q_I \rangle / \langle q_B \rangle$ as functions of x_G and x_D for the two mixtures. The red line with open circles and the blue line with filled circles represent for GW and DW mixtures, respectively. Horizontal dashed blue line in panel (c) indicates $\langle q_I \rangle / \langle q_B \rangle = 1$. Note that these calculations are done by considering the nearest four solvent molecules (both water and cosolvents) from a central water molecule.

at slightly higher than unity. The scenario is again different for the DW mixture. As visible in both Figs. 4(b) and 5(b), $\langle q_I \rangle$ at the interface decrease more than $\langle q_B \rangle$ in bulk with the same increase of x_D. Therefore the ratio, presented in Fig. 5(c), decreases from slightly higher than 1.0 for neat water to ~0.95 at $x_D = 0.15$. The above observations clearly indicate that while glycerol affects the tetrahedral order of the interfacial and the bulk water solvent almost uniformly, DMSO's influence is not uniform. A more meticulous comparison between Figs. 5(a) and 5(b) reveals an interesting picture. At $x_G = 0.15$, the value of $\langle q_I \rangle$ at the interface (0.62) is higher than the value (0.59) at the same mole fraction for the DW mixture. On the other hand, the $\langle q_B \rangle$ value (0.62) for GW mixture at $x_G = 0.15$ is almost the same with the $\langle q_B \rangle$ value for DW mixture at $x_D = 0.15$. Consequently, the glycerol and DMSO cosolvents perturb the three-dimensional tetrahedral H-bonding network of water near the hydrophobic solute almost similarly at the bulk limit, but the effect on the interfacial water solvent is not akin. DMSO disrupts the orientational order of interfacial water more intensely. This observation gives the signature of stronger possible preferential interaction between the hydrophobic solute and DMSO cosolvent. We will return to this discussion in Sec. III D.

B. H-bonding of water

In order to elucidate further on how the two cosolvents relatively affect H-bonding between water molecules at the hydrophobic interface and the bulk, we calculate the number of H-bonds per water molecule (N_h) as a function of distance from the solute.

Figures 6(a) and 6(b) exhibit N_h as a function of distance from the solute for 4 different compositions ($x = 0.0, 0.05, 0.10$, and 0.15) for each of the GW and the DW binary mixtures. We have adopted the widely accepted H-bond criteria ($r_{O_DO_A}$ < 3.5 Å, $r_{O_AH_D}$ < 2.45 Å, $H_DO_DO_A$ < 30°, where "D" and "A" stand for the H-bond donor and acceptor, respectively). Noticeably, for neat liquid water, N_h goes to the maximum at r_{XeO_W} ~ 4.5 Å distance from the solute and then after some undulation it almost levels off beyond r_{XeO_W} = 10 Å distance. The peak at r_{XeO_W} ~ 4.5 Å distance indicates stronger water H-bonding network at the solute-water interface. This result is consistent with the earlier observations of stronger water H-bonding near the hydrophobic interface than that in the bulk.[73] Figure 6(a) shows that for GW binary mixtures, N_h decreases steadily with increasing x_G at all the distances from the solute. To see the relative perturbation by the cosolvents at the interface and the bulk regions, we have plotted the ratio N_h^I/N_h^B in Fig. 6(c). Here, N_h^I and N_h^B are, respectively,

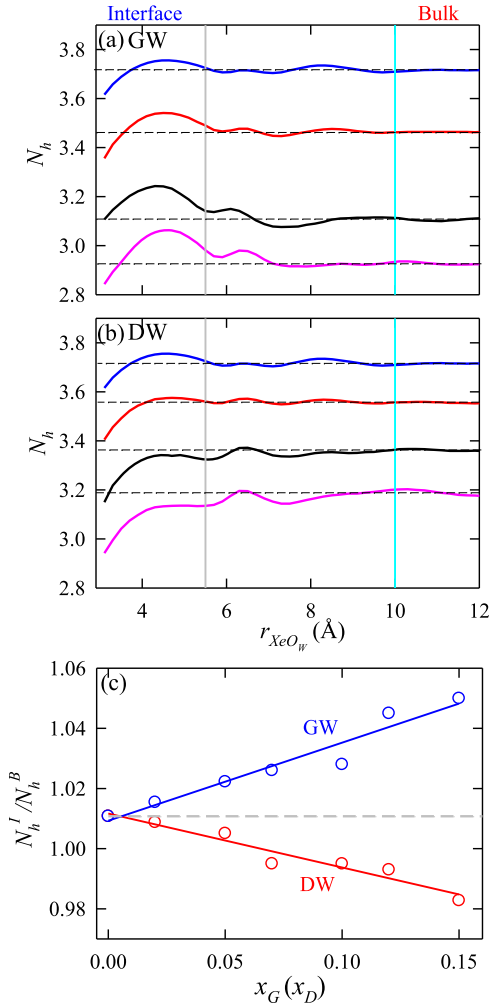

FIG. 6. [(a) and (b)] Number of water···water H-bonds per water molecule (N_h) as a function of distance from the solute for GW mixtures [panel (a)] and DW mixtures [panel (b)]. The data for only 4 different compositions (x = 0.0, 0.05, 0.10, 0.15) are shown here. (c) The ratio between N_h at the interface ($N_h{}^I$) and N_h at the bulk ($N_h{}^B$). The solid lines in panel (c) are the linear fits of the data. The vertical lines in panels (a) and (b) indicate the upper limit of the interface (1st hydration shell) and the lower limit of the bulk region. The horizontal dashed lines in panels (a) and (b) indicate the bulk values of the corresponding compositions of the two mixtures. The horizontal dashed line in panel (c) indicates the ratio ($N_h{}^I/N_h{}^B$) for pure water.

the first peak height and the average value of N_h at the bulk region. Clearly, the ratio increases with x_G. This suggests that the increased number of glycerol molecules draw more water molecules at the interfacial region from the outer solvation layers. Hence, the ratio N_h^I/N_h^B increases with increasing glycerol concentration in the mixture. However, we have already witnessed in Fig. 3 that relative "tetrahedrality" ($\langle q_I\rangle/\langle q_B\rangle$) of solvent remains almost insensitive to x_G. Thus glycerol, on the one hand, uniformly disrupts the local tetrahedral H-bonding structure of water at both the bulk and interface and, on the other hand, it retains some water···water H-bonds in the solute's first hydration shell. This is an excellent scenario for stabilization of protein at low temperature.

The overall decrease of N_h with increasing DMSO concentration in the DW mixture is evidenced in Fig. 6(b). However, the situation is substantially different here compared to the GW mixture. As seen in Fig. 6(c), the ratio (N_h^I/N_h^B) decreases with an increase in x_D. This indicates that DMSO molecules disturb the H-bond structure of the interfacial water molecules more strongly than that of the bulk water molecules in the DW mixture. Also, as we have seen in Fig. 3, the local tetrahedral structure of hydrophobic interfacial water is disrupted more than that in bulk. Therefore, DMSO decreases both the number of water···water H-bonding and the local tetrahedral H-bonding network. This can be one of the possible reasons of why protein gets precipitated in high DMSO concentration in solution.

We have repeated the above analysis but considering both water and cosolvent as H-bond partners of the central water molecule. Similar results are obtained. The results are presented in Fig. S3 of the supplementary material. It is worth mentioning that the decrease of the overall H-bonding interaction with increasing the cosolvent concentration can explain the stability of hydrophobic-interaction-induced self-assembly structures, like proteins. This is due to the theory, described in Ref. 53, which states that cold denaturation of protein can occur naturally because of increasing strength of interfacial water···water hydrogen bond interaction.

C. Radial distribution of water solvent around the solute

In Secs. III A and III B, we found strong indication that glycerol draws more water molecules at the solute/water interface from bulk and DMSO excludes water solvent from the interface. To obtain more conclusive evidence, we look at the mass density of water (ρ_w) as a function of distance from the solute for GW and DW mixtures. Figures 7(a) and 7(b) present ρ_w as a function of distance from the solute at 4 different compositions of GW and DW mixtures, respectively.

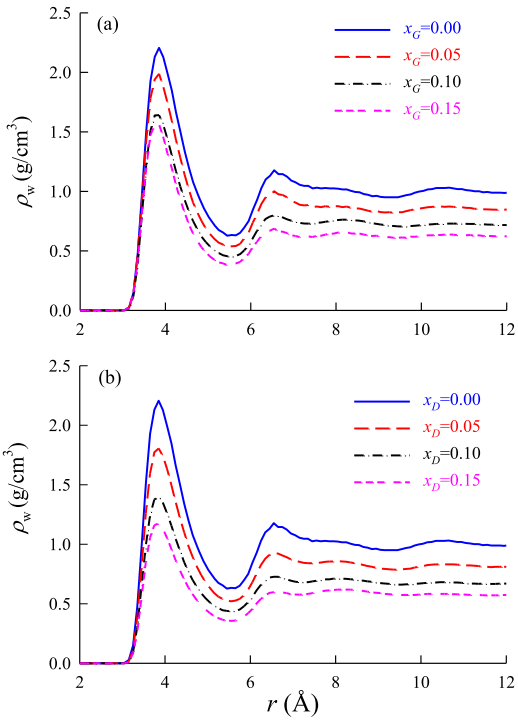

FIG. 7. Density of water as a function of distance from the solute for 4 different compositions of the two binary mixtures: (a) GW and (b) DW. The results are shown here only for 4 compositions of each of the mixtures.

While ρ_w peaks at $r \sim 4.0$ Å distance from the solute, the first minimum arises at $r \sim 5.5$ Å. The density almost levels off after 10 Å distance from the solute, which is the bulk regime. With increasing concentration of glycerol and DMSO in the GW and the DW mixture, respectively, the density of water decreases at all regions varying the distance from the solute. This is pretty straightforward since the total number of water molecules decreases with increasing glycerol or DMSO concentration. However, the question remains whether the density of water decreases uniformly at all regions around the solute. We discuss this now.

Figure 8(a) exhibits the density of the interfacial water solvent ρ_I (the first peak intensities) and the bulk water ρ_B as a function of glycerol and DMSO concentration for GW and DW binary mixtures, respectively. For GW mixture, while ρ_I decreases from ~2.2 (for neat water) to ~1.6 (at $x_G = 0.15$), ρ_B decreases from ~1.0 (for neat water) to ~0.6 (at $x_G = 0.15$). Therefore, the reduction of water density at the interface (~27%) is less than that at the bulk (~40%). On the other hand for the DW mixture, while the first peak intensity decreases from ~2.2 (for neat water) to ~1.2 (at $x_D = 0.15$), the bulk water density decreases from ~1.0 (for neat water) to ~0.6 (at $x_D = 0.15$). Therefore, the interfacial water solvent density decreases by 45% for the DW mixture at $x_D = 0.15$. This reduction is almost twice the reduction of the interfacial water solvent density for the same increase in the glycerol concentration.

Figure 8(b) plots the ratio ρ_I/ρ_B as a function of the concentration of glycerol and DMSO for the GW and DW binary mixtures, respectively. Interestingly, the ratio increases with increasing x_G for GW binary mixtures. In contrast, the ratio decreases with DMSO concentration in the DW mixture. This provides an absolutely clear picture that glycerol attracts solvent water molecules from the bulk region at a higher concentration of glycerol and thereby prevents complete drying out of water from the first hydration shell of the hydrophobic solute. In addition, glycerol acts as a good anti-freezing substance by disrupting both the local tetrahedral structure and water···water H-bonding network. Glycerol, therefore, endorses two level protections of living cells and biomolecules at the extreme condition. On the other hand, DMSO excludes water molecules from the first hydration shell at higher concentration of DMSO. These are consistent with the changes of the H-bond numbers per water molecule in these mixtures as a function of cosolvent concentration. Clearly, at high concentration of DMSO, water density becomes significantly low near the solute and therefore DMSO is not a very good cosolvent for stabilizing biomolecules at the extreme condition particularly at a high concentration of the DMSO mixture. This is consistent with experimental observation.[58]

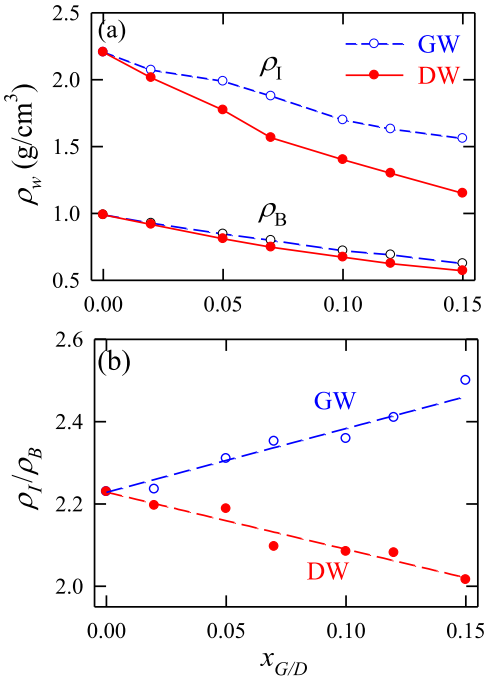

FIG. 8. (a) The densities of the interfacial water molecules (ρ_I) and the bulk water molecules (ρ_B) as a function of glycerol and DMSO concentration for GW (blue dashed lines) and DW (red solid lines) binary mixture, respectively. (b) The ratio, ρ_I/ρ_B, as a function of the composition of the two mixtures. The dashed lines in panel (b) are the linear fits of the data.

D. Hydrophobic effect and orientational ordering of the cosolvents

In Secs. III A–III C, we observed the contrasting roles of glycerol and DMSO on the structural disruption of water solvent's orientational and H-bond structure at the hydrophobic interface and in the bulk region. While glycerol affects the regular tetrahedral H-bonding structure of water almost uniformly at all regions, DMSO's role is somewhat non-uniform since the latter affects the interfacial water structure more intensely than the bulk water. These results corroborate with the observations from earlier studies. In this section, we focus on the plausible mechanism for the above contrasting behaviors of these two cosolvents. We see whether the contrasting behavior is somehow correlated with the intrinsic molecular structures of these two cosolvents.

Here, we examine the orientational distribution of the key segments of the two cosolvents at different distances from the hydrophobic solute. Figure 9(b) exhibits two-dimensional probability density distribution ($P(r,\theta)$) of the angles θ—between glycerol C_T···Xe vector and the glycerol C_G—C_T bond vector [see Fig. 9(a) for the atom labels]—and the distance r_{XeC_T} between the Xe atom and the glycerol C_T atom for the GW mixture with $x_G = 0.10$, as a representative composition. The distribution has a high-intensity peak at r_{XeC_T} = 3.5 Å and $\theta = 0°$ angle. Therefore, the terminal CH_2 groups align toward the hydrophobic solute. This is due to the hydrophobic interaction between the CH_2 groups of glycerol and the Xe solute.

Now, we study the orientational alignment of the hydroxyl groups of the glycerol molecules. We have plotted—in Fig. 9(c)—$P(r,\phi)$ as functions of the angle ϕ {between the glycerol OH—H bond vector and glycerol OH···Xe vector [see Fig. 9(a) for the atom labels]} and the distance r_{XeOH} (between the Xe atom and the OH atom of the glycerol molecule) for the GW mixture with $x_G = 0.10$. Note that similar pictures (not shown here) are seen for other compositions. In the interfacial region ($r_{XeOH} < 5.5$ Å), the distribution has two maxima: one at $\phi = 70°$ and the other one at $\phi = 180°$. Therefore,

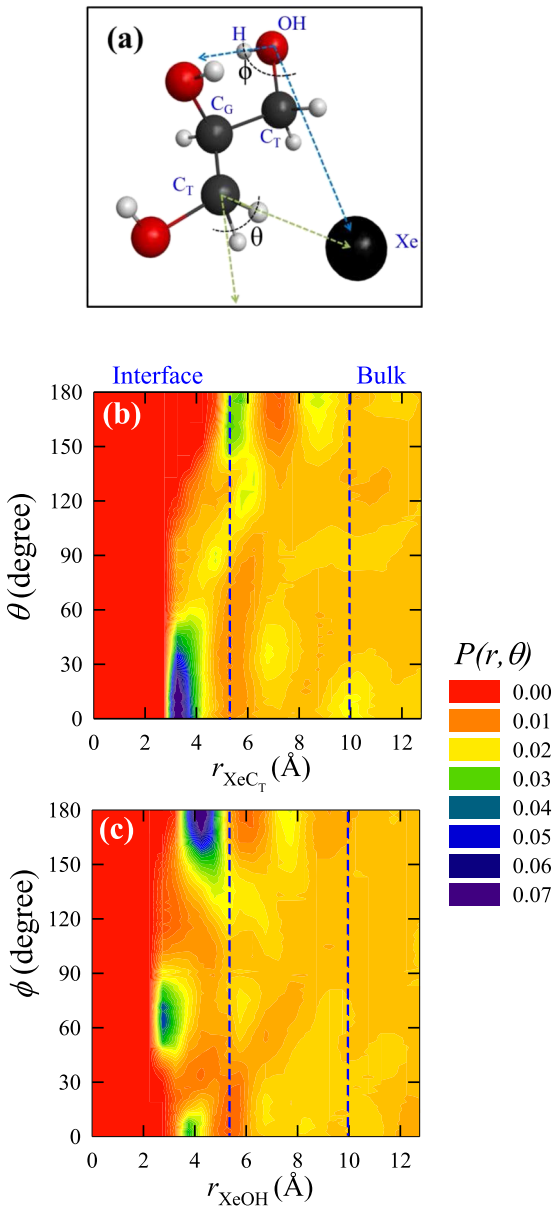

FIG. 9. (a) Schematic diagrams of a glycerol molecule and the Xe solute. The angle θ between the C_T—Xe vector and the C_G—CT bond vector and the angle ϕ between the glycerol OH—H vector and glycerol OH—Xe vector are indicated. (b) Two-dimensional probability density distribution ($P(r,\theta)$) of the angle θ and the distance between Xe and the C_T atom of the glycerol molecule (r_{XeC_T}) for the GW mixture at a representative mole fraction x_G = 0.10. (c) Two-dimensional probability density distribution ($P(r,\phi)$) of the angle ϕ and the distance between Xe and the O atom of the glycerol molecule (r_{XeOH}) for the GW mixture at a representative mole fraction x_G = 0.10. The vertical dashed lines in all panels indicate the interfacial and bulk regions.

the majority of the OH groups of the glycerol molecules are either aligned tangentially to the hydrophobic solute surface or they are aligned toward the bulk region. Apparently, this angular arrangement of glycerol's hydroxyl groups is very similar to the angular arrangement of water OH bonds in the hydrophobic interfacial region. The latter is presented in Fig. S4 of the supplementary material. Majority of the water OH bonds are aligned either tangential to the solute surface or are directed toward the bulk water molecules. Therefore, the glycerol OH groups would participate in both tangential and bulk H-bonding with solvent water molecules. (See Fig. S5 of the supplementary material.) This water-like orientational arrangement is the possible factor, which does not allow the glycerol molecules to discriminate between the interfacial and the bulk water molecules while perturbing the tetrahedral H-bond structure of water.

Now we turn our focus on the orientational arrangement of DMSO molecules around the solute. Figure 10(b) exhibits two-dimensional probability density distribution ($P(r, \theta)$) of the angle θ—between the DMSO CD—Xe vector and DMSO S—CD bond vector—and the distance r_{XeCD}—between the Xe atom and DMSO CD atom—for the DW mixture with x_D = 0.10, as a representative one. r_{XeCD} and θ are labeled in Fig. 10(a). Note that similar pictures (not shown here) are seen

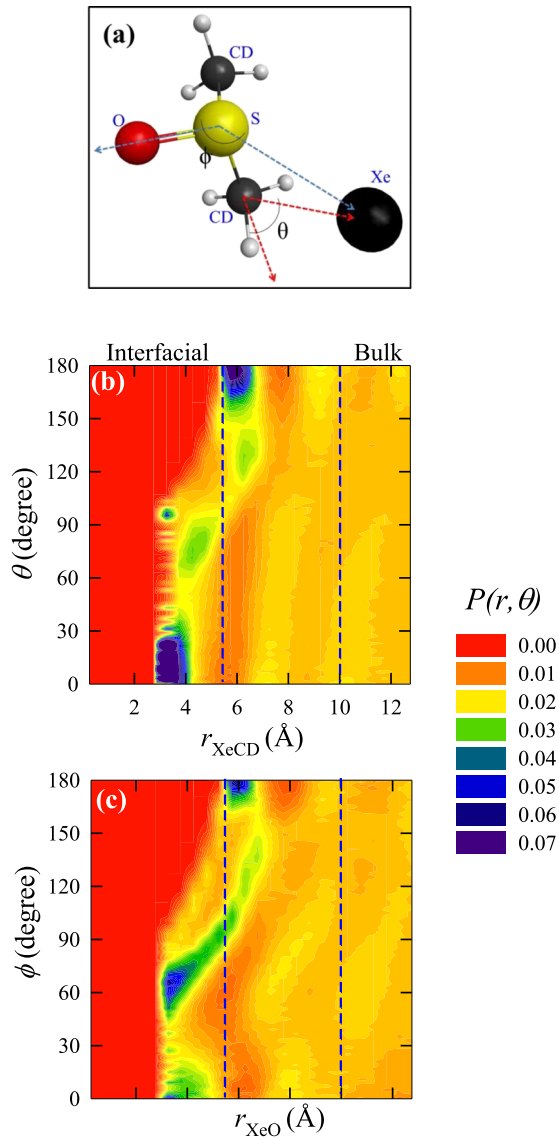

FIG. 10. (a) Schematic diagrams of a DMSO molecule and the Xe solute. The angle θ between the CD—Xe vector and the S—CD bond vector and the angle ϕ between the DMSO S=O vector and S—Xe vector are indicated. (b) Two-dimensional probability density distribution ($P(r,\theta)$) of the angle θ and the distance between Xe and the CD atom of DSMO molecule (r_{XeCD}) for the DW mixture at a representative mole fraction x_D = 0.10. (c) Two-dimensional probability density distribution ($P(r,\phi)$) of the angle ϕ and the distance between Xe and the O atom of DSMO molecule (r_{XeO}) for the DW mixture at a representative mole fraction x_D = 0.10. The vertical dashed lines in panels (b) and (c) indicate the interfacial and bulk regions.

for other compositions. The peak is centered at $\theta = 0°$ angle and $r_{XeCD} = 3.5$ Å distance from the solute. Therefore—similar to the alignment of terminal CH_2 groups of interfacial glycerol molecules—the methyl groups of DMSO are also directed toward the hydrophobic Xe solute. This gives a strong indication of hydrophobic interaction between the DMSO's methyl groups and the Xe solute.

Finally, we focus on the angular alignment of the S=O groups of the DMSO cosolvent molecules in the proximity of the solute. Figure 10(c) plots $P(r,\phi)$ as a function of the angle ϕ—between the DMSO S$\cdots$Xe vector and DMSO S=O bond vector [see Fig. 10(a) for the labels]—and the distance r_{XeO}—between the Xe atom and DMSO O atom—for the DW mixture having $x_D = 0.10$, as a representative one. Clearly, for the interfacial DMSO molecules $P(r,\phi)$ peaks at $\phi \sim 65°$. This indicates that the S=O groups of the interfacial DMSO molecules are aligned tangentially to the solute. Therefore, these S=O groups will involve in H-bonding only with water$\cdots$water tangential H-bonds and thereby selectively affect the tangential H-bonding structure of the water solvent in the close proximity of the Xe solute. We have shown in Fig. S5 of the supplementary material that the glycerol cosolvent molecules affect both the tangential and the bulk H-bonding of interfacial water solvent molecules, while DMSO molecules selectively affect the tangential H-bonds. Note that these tangential water$\cdots$water H-bonds are a unique identity of the water hydrophobic interfacial region. Therefore, the selective attacking of the tangential H-bonds by DMSO molecules perturbs the interfacial hydration layer very differently than that in bulk. On the other hand, glycerol molecules behave very similar to those of solvent water molecules in terms of H-bonding with solvent water. These emphasize why glycerol influences the water solvent structure uniformly at all regions, but DMSO has preferential influence on interfacial water solvent structure.

IV. CONCLUSIONS

In this paper, we have systematically studied the effect of two well-known cryoprotectants—glycerol and DMSO—on the local tetrahedral order of water molecules at −5 °C adjacent to a hydrophobic solute and at the bulk region. We have found a steady reduction of tetrahedral order and the number of water$\cdots$water H-bonds per water molecule at both the bulk and hydrophobic interface with increasing concentration of glycerol and DMSO in water. Contrasting roles of glycerol and DMSO have been clearly evidenced. While the interfacial and bulk tetrahedral H-bonding networks of water are affected by glycerol almost uniformly, DMSO disrupts the water structure around the nonpolar solute in a nonhomogeneous way. DMSO selectively affects the interfacial water structure more than that of the bulk water. Also, the presence of glycerol cosolvent in the mixture does not allow a complete drying out of the interface by retaining some water molecules in this region. Note that this cosolvent induced water retaining is the key for protein stabilization against denaturation. In contrast, the stronger hydrophobic interaction between hydrophobic methyl residues of DMSO and the hydrophobic solute replaces water molecules from the interface. This provides somewhat clear indications that glycerol has more efficacy for stabilizing protein than DMSO in aqueous solution. This is consistent with previous studies.[56–64] The contrasting role of glycerol and DMSO on disrupting the local order of interfacial water has been connected with hydrophobic interaction (between the solute and the cosolvents) induced orientation of the cosolvents adjacent to the hydrophobic solute. While glycerol has three hydroxyl groups, forming strong HBs with solvent water by both accepting and donating H-bonds, DMSO can only accept the H-bond from water solvents. Therefore, the glycerol molecules behave almost like water solvent (in terms of H-bonding structure) and therefore can act as water replacement with minimal distortion of the overall H-bond network near the hydrophobic interface.

Finally, this work has mainly focused on the disruption of the tetrahedral structure of liquid water at the hydrophobic interface relative to the bulk. However, it is also essential to know how these cosolvents affect the dynamics of water molecules in different regions from the solute. The results of this work will be presented separately elsewhere.

SUPPLEMENTARY MATERIAL

See supplementary material for (i) a table detailing compositions and simulated densities of different mixtures, (ii) solute-solvent radial distribution function, (iii) plot of the number of H-bonds per water molecule as a function of distance from the solute, (iv) two-dimensional probability density distribution ($P(r,\theta)$) of the angles θ—between the water $O_W\cdots Xe$ vector and the water O_W—H_W bond vector—and the distance r_{XeC_T}—between the Xe atom and the glycerol C_T atom for the GW mixture—with $x_G = 0.10$, and (v) angular distribution of cosolvent-water H-bond at the interface.

ACKNOWLEDGMENTS

I acknowledge Dr. Sandipa Indra for various suggestions. I acknowledge the Indian Institute of Technology Patna for computational facilities and financial assistance.

The author declares no competing financial interest.

[1] J. L. Dashnau, N. V. Nucci, K. A. Sharp, and J. M. Vanderkooi, J. Phys. Chem. B **110**, 13670 (2006).
[2] J. J. Towey, A. K. Soper, and L. Dougan, J. Phys. Chem. B **120**, 4439 (2016).
[3] J. J. Towey, A. K. Soper, and L. Dougan, J. Phys. Chem. B **116**, 13898 (2012).
[4] J. J. Towey and L. Dougan, J. Phys. Chem. B **116**, 1633 (2012).
[5] D. B. Wong, K. P. Sokolowsky, M. I. El-Barghouthi, E. E. Fenn, C. H. Giammanco, A. L. Sturlaugson, and M. D. Fayer, J. Phys. Chem. B **116**, 5479 (2012).
[6] B. Kirchner and M. Reiher, J. Am. Chem. Soc. **124**, 6206 (2002).
[7] K.-I. Oh, K. Rajesh, J. F. Stanton, and C. R. Baiz, Angew. Chem., Int. Ed. **56**, 11375 (2017).
[8] A. K. Soper and A. Luzar, J. Chem. Phys. **97**, 1320 (1992).
[9] A. K. Soper and A. Luzar, J. Phys. Chem. **100**, 1357 (1996).
[10] M. R. Harpham, N. E. Levinger, and B. M. Ladanyi, J. Phys. Chem. B **112**, 283 (2008).
[11] C. Chen, W. Z. Li, Y. C. Song, and J. Yang, J. Mol. Liq. **146**, 23 (2009).
[12] L. Weng, C. Chen, J. Zuo, and W. Li, J. Phys. Chem. A **115**, 4729 (2011).
[13] J. Bachler, V. Fuentes-Landete, D. A. Jahn, J. Wong, N. Giovambattista, and T. Loerting, Phys. Chem. Chem. Phys. **18**, 11058 (2016).
[14] A. V. Egorov, A. P. Lyubartsev, and A. Laaksonen, J. Phys. Chem. B **115**, 14572 (2011).

[15]N. Engel, K. Atak, K. M. Lange, M. Gotz, M. Soldatov, R. Golnak, E. Suljoti, J.-E. Rubensson, and E. F. Aziz, J. Phys. Chem. Lett. **3**, 3697 (2012).
[16]A. Perera and R. Mazighi, J. Chem. Phys. **143**, 154502 (2015).
[17]S. Indra and R. Biswas, J. Phys. Chem. B **120**, 11214 (2016).
[18]P. B. Conrad and J. J. de Pablo, J. Phys. Chem. A **103**, 4049 (1999).
[19]I. I. Vaismant and M. L. Berkowitz, J. Am. Chem. Soc. **114**, 7889 (1992).
[20]S. Chowdhuri and A. Chandra, J. Chem. Phys. **119**, 4360 (2003).
[21]A. Luzar and D. Chandler, J. Chem. Phys. **98**, 8160 (1993).
[22]C. Branden and J. Tooze, *Introduction to Protein Structures*, 2nd ed. (Taylor and Francis, London, 1999).
[23]T. E. Creighton, *Proteins*, 2nd ed. (Freeman, New York, 1999).
[24]C. O. Fagain, *Protein Stability and Stabilization of Protein Function* (Landes Bioscience, Georgetown, TX, 1997).
[25]S. A. Hawley, Biochemistry **10**, 2436 (1971).
[26]P. L. Privalov, J. Chem. Thermodyn. **29**, 447 (1997).
[27]R. Kitahara, A. Okuno, M. Kato, Y. Taniguchi, S. Yokoyama, and K. Akasaka, Magn. Reson. Chem. **44**, S108–S113 (2006).
[28]D. Sanfelice and P. A. Temussi, Biophys. J. **208**, 4 (2016).
[29]P. L. Privalov, Crit. Rev. Biochem. Mol. Biol. **25**, 281 (1990).
[30]A. Pastore, S. R. Martin, A. Politou, K. C. Kondapalli, T. Stemmler, and P. A. Temussi, J. Am. Chem. Soc. **129**, 5374 (2007).
[31]V. R. Agashe and J. B. Udgaonkar, Biochemistry **34**, 3286 (1995).
[32]P. L. Privalov, Y. V. Griko, S. Y. Venyaminov, and V. P. Kutyshenko, J. Mol. Biol. **190**, 487 (1986).
[33]C. Yang, S. Jang, and Y. Pak, Nat. Commun. **5**, 5773 (2014).
[34]C. L. Dias, T. Ala-Nissila, J. Wong-ekkabut, I. Vattulainen, M. Grant, and M. Karttunen, Cryobiology **60**, 91 (2010).
[35]F. Franks, R. H. M. Hatley, and H. L. Friedman, Biophys. Chem. **31**, 307 (1988).
[36]F. Franks, Adv. Protein Chem. **46**, 105 (1995).
[37]B. L. Chen and J. A. Schellman, Biochemistry **28**, 685 (1989).
[38]B. Hallerbach and H. J. Hinz, Biophys. Chem. **76**, 219 (1999).
[39]C. L. Dias, T. Ala-Nissila, M. Karttunen, I. Vattulainen, and M. Grant, Phys. Rev. Lett. **100**, 118101 (2008).
[40]M. Marqués, J. M. Borreguero, H. E. Stanley, and N. V. Dokholyan, Phys. Rev. Lett. **91**, 138103 (2003).
[41]M. Davidovic, C. Mattea, J. Qvist, and B. Halle, J. Am. Chem. Soc. **131**, 1025 (2009).
[42]D. Sanfelice, E. Morandi, A. Pastore, N. Niccolai, and P. A. Temussi, ChemPhysChem **16**, 3599 (2015).
[43]C. J. Tsai, J. V. Maizel, Jr., and R. Nussinov, Crit. Rev. Biochem. Mol. Biol. **37**, 55 (2002).
[44]C. F. Lopez, R. K. Darst, and P. J. Rossky, J. Phys. Chem. B **112**, 5961 (2008).
[45]J. R. Grigera and A. N. McCarthy, Biophys. J. **98**, 1626 (2010).
[46]E. Ascolese and G. Graziano, Chem. Phys. Lett. **467**, 150 (2008).
[47]M. Maiti, S. Weiner, S. V. Buldyrev, H. E. Stanley, and S. Sastry, J. Chem. Phys. **136**, 044512 (2012).
[48]C. L. Dias, Phys. Rev. Lett. **109**, 048104 (2012).
[49]S. Parui and B. Jana, J. Phys. Chem. B **121**, 7016 (2017).
[50]S. B. Kim, J. C. Palmer, and P. G. Debendetti, Proc. Natl. Acad. Sci. U. S. A. **113**, 8991 (2016).
[51]T. Hajari and S. Bandyopadhyay, J. Chem. Phys. **146**, 225104 (2017).
[52]A. Ben-Naim, Adv. Biol. Chem. **3**, 29 (2013).
[53]V. Bianco and G. Franzese, Phys. Rev. Lett. **115**, 108101 (2015).
[54]M. E. Johnson, C. Malardier-Jugroot, and T. Head-Gordon, Phys. Chem. Chem. Phys. **12**, 393 (2010).
[55]A. M. Schrader, C.-Y. Cheng, J. N. Israelachvili, and S. Han, J. Chem. Phys. **145**, 041101 (2016).
[56]K. Gekko and S. N. Timasheff, Biochemistry **20**, 4667 (1981).
[57]V. Vagenende, M. G. S. Yap, and B. L. Trout, Biochemistry **48**, 11084 (2009).
[58]S. Bhattacharjya and P. Balaram, Proteins **29**, 492 (1997).
[59]K. Hamaguchi, J. Biochem. **56**, 441 (1964).
[60]P. Huang, A. Dong, and W. S. Caughey, J. Pharmacol. Sci. **84**, 387 (1995).
[61]T. Kamiyama, T. Matsusita, and T. Kimura, J. Chem. Eng. Data **48**, 1301 (2003).
[62]S. Roy, B. Jana, and B. Bagchi, J. Chem. Phys. **136**, 115103 (2012).
[63]S. Roy and B. Bagchi, J. Phys. Chem. B **117**, 4488 (2012).
[64]S. Roy and B. Bagchi, J. Chem. Phys. **139**, 034308 (2013).
[65]D. T. Bowron, A. Filipponi, M. A. Roberts, and J. L. Finney, Phys. Rev. Lett. **81**, 4164 (1998).
[66]H. S. Ashbaugh, D. Asthagiri, L. R. Pratt, and S. B. Rempe, Biophys. Chem. **105**, 323 (2003).
[67]N. Galamba, J. Phys. Chem. B **117**, 2153 (2013).
[68]N. Galamba, J. Phys. Chem. B **118**, 4169 (2014).
[69]N. Galamba, J. Phys. Chem. B **117**, 589 (2013).
[70]B. Lee, Biopolymers **24**, 813 (1985).
[71]R. L. Baldwin, Proc. Natl. Acad. Sci. U. S. A. **111**, 13052 (2014).
[72]J. T. Titantah and M. Karttunen, J. Am. Chem. Soc. **134**, 9362 (2012).
[73]J. Grdadolnika, F. Merzela, and F. Avbelj, Proc. Natl. Acad. Sci. U. S. A. **114**, 322 (2017).
[74]V. I. Artyukhov, A. Yu. Pulver, A. Peregudov, and I. Artyuhov, J. Chem. Phys. **141**, 034503 (2014).
[75]R. Haselmeier, M. Holz, W. Marbach, and H. Weingärtner, J. Phys. Chem. **99**, 2243 (1995).
[76]D. Paschek, J. Phys. Chem. **120**, 6674 (2004).
[77]O. Coskuner and U. K. Dieters, Z. Phys. Chem. **221**, 785 (2007).
[78]K. Lum, D. Chandler, and J. D. Weeks, J. Phys. Chem. B **103**, 4570 (1999).
[79]D. M. Huang and D. Chandler, Proc. Natl. Acad. Sci. U. S. A. **97**, 8324 (2000).
[80]H. S. Ashbaugh and M. E. Paulaitis, J. Am. Chem. Soc. **123**, 10721 (2001).
[81]S. Rajamani, T. M. Truskett, and S. Garde, Proc. Natl. Acad. Sci. U. S. A. **102**, 9475 (2005).
[82]H. S. Ashbaugh and L. R. Pratt, Rev. Mod. Phys. **78**, 159 (2006).
[83]M. V. Athawale, S. N. Jamadagni, and S. Garde, J. Chem. Phys. **131**, 115102 (2009).
[84]S. Garde and A. J. Patel, Proc. Natl. Acad. Sci. U. S. A. **108**, 16491 (2011).
[85]C. Camilloni, D. Bonetti, A. Morrone, R. Giri, C. M. Dobson, M. Brunori, S. Gianni, and M. Vendruscolo, Sci. Rep. **6**, 28285 (2016).
[86]R. V. Rariy and A. M. Klibanov, Proc. Natl. Acad. Sci. U. S. A. **94**, 13520 (1997).
[87]T. Arakawa, Y. Kita, and S. N. Timasheff, Biophys. Chem. **131**, 62 (2007).
[88]J. Wang, R. M. Wolf, J. W. Caldwell, P. A. Kollman, and D. A. Case, J. Comput. Chem. **25**, 1157 (2004).
[89]R. Chelli, P. Procacci, G. Cardini, R. G. DellaValle, and S. Califano, Phys. Chem. Chem. Phys. **1**, 871 (1999).
[90]J. Blieck, F. Affouard, P. Bordat, A. Lerbret, and M. Descamps, Chem. Phys. **317**, 253 (2005).
[91]J. L. F. Abascal and C. Vega, J. Chem. Phys. **123**, 234505 (2005).
[92]F. O. Akinkunmi, D. A. Jahn, and N. Giovambattista, J. Phys. Chem. B **119**, 6250 (2015).
[93]M. L. Strader and S. E. Feller, J. Phys. Chem. A **106**, 1074 (2002).
[94]A. D. Becke, Phys. Rev. A **38**, 3098 (1988).
[95]C. Lee, W. Yang, and R. G. Parr, Phys. Rev. B **37**, 785 (1988).
[96]M. J. Frisch, G. W. Trucks, H. B. Schlegel, G. E. Scuseria, M. A. Robb, J. R. Cheeseman, G. Scalmani, V. Barone, B. Mennucci, and G. A. Petersson, GAUSSIAN 09, Revision B.01, Gaussian, Inc., Wallingford, CT, 2010.
[97]L. Martínez, R. E. Andrade, G. Birgin, and J. M. Martínez, J. Comput. Chem. **30**, 2157 (2009).
[98]D. van der Spoel, E. Lindahl, B. Hess, G. Groenhof, A. E. Mark, and H. J. C. Berendsen, J. Comput. Chem. **26**, 1701 (2005).
[99]S. A. Nosé, J. Chem. Phys. **81**, 511 (1984).
[100]W. G. Hoover, Phys. Rev. A **31**, 1695 (1985).
[101]H. J. C. Berendsen, J. P. M. Postma, W. F. van Gunsteren, A. DiNola, and J. R. Haak, J. Chem. Phys. **81**, 3684 (1984).
[102]M. R. Shirts, J. Chem. Theory Comput. **9**, 909 (2013).
[103]M. Parrinello and A. Rahman, J. Appl. Phys. **52**, 7182 (1981).
[104]S. A. Schichman and R. A. Amey, J. Phys. Chem. **75**, 98 (1971).
[105]N. Giovambattista, P. G. Debenedetti, F. Sciortino, and H. E. Stanley, Phys. Rev. E **71**, 061505 (2005).
[106]Z. Yan, S. V. Buldyrev, P. Kumar, N. Giovambattista, P. Debenedetti, and H. Stanley, Phys. Rev. E **76**, 051201 (2007).
[107]S. Chatterjee, P. G. Debenedetti, F. H. Stillinger, and R. M. Lynden-Bell, J. Chem. Phys. **128**, 124511 (2008).
[108]D. R. Nutt and J. C. Smith, J. Am. Chem. Soc. **130**, 13066 (2008).
[109]M. Paolantoni, N. F. Lago, M. Albertí, and M. A. Lagana, J. Phys. Chem. A **113**, 15100 (2009).
[110]E. Dubouev-Dijon and D. Laage, J. Phys. Chem. B **119**, 8406 (2015).
[111]S. Indra and S. Daschakraborty, Chem. Phys. Lett. **685**, 322 (2017).